Reprinted from *J. Mol. Biol.* (1981) **146**, 119–141

Conformational and Geometrical Properties of β-Sheets in Proteins

II. Antiparallel and Mixed β-Sheets

F. R. Salemme and D. W. Weatherford

J. Mol. Biol. (1981) **146**, 119–141

Conformational and Geometrical Properties of β-Sheets in Proteins

II. Antiparallel and Mixed β-Sheets

F. R. SALEMME AND D. W. WEATHERFORD

Department of Biochemistry
New Chemistry Building
University of Arizona, Tucson, Ariz. 85721, U.S.A.

(Received 9 October 1979, and in revised form 17 September 1980)

The present work treats the conformational and geometrical properties of antiparallel and mixed β-sheets, following the approach described in the first paper of this series (Salemme & Weatherford, 1981). As shown, antiparallel structures possess conformational degrees of freedom that allow them to assume a greater diversity of spatial configurations than occur in parallel sheets. This configurational flexibility principally owes its origin to the potential variability of the interchain hydrogen bond geometry in antiparallel structures. As a consequence of this inherent elasticity of antiparallel β-sheets, their extended spatial configurations strongly reflect effects arising from local or extended side-chain packing interactions. Although the continuously deformable characteristics of antiparallel sheets frequently result in the attainment of spatial configurations that cannot be quantitatively modeled as hydrogen-bonded arrays of conformationally identical polypeptide chains, several observed sheets are nevertheless shown to be accurately approximated as conformationally regular arrays that typically yield model *versus* observed fits of less than 1 Å for corresponding α-carbon atoms.

1. Introduction

The regularly hydrogen-bonded antiparallel β-sheets observed in globular proteins show considerably more geometrical diversity than is generally observed in parallel sheets. These differences might in principle be ascribed to environmental effects: i.e. whereas extended parallel sheets are generally located on the interior of globular proteins where they constitute a structural framework upon which remaining structural elements of the protein pack, antiparallel sheets are frequently observed to additionally constitute either exterior surfaces or isolated structural domains in proteins (Richardson, 1977). This paper examines the conformational and geometrical properties of extended antiparallel and mixed β-sheets and describes how the conformational restrictions associated with the optimal preservation of interchain hydrogen bonding manifest themselves in the observed geometrical properties of these structures.

0022-2836/81/050119-23 $02.00/0

2. Methods

The computational approach utilized for the generation and examination of regular antiparallel sheet model structures follows that described for parallel structures (Salemme & Weatherford, 1981), with one important exception. As described previously, the optimal hydrogen-bonding geometry for parallel β-sheets is one in which the NOC interchain hydrogen bond is linear. This is not necessarily the case in antiparallel structures where, owing to the presence of local dyad axes of symmetry perpendicular to the plane of the sheet, the hydrogen bonds may be symmetrically and isoenergetically bent at the carbonyl oxygen (Raghavendra & Sasisekharan, 1979). Consequently, the analysis of the conformational properties of antiparallel structures incorporated a variety of representative hydrogen-bond geometries that differed in their C–O–N hydrogen bond angle.

Co-ordinates for model structures of extended β-sheets used for comparison with observed protein structures were generated by least-squares rotation of appropriate substructures (e.g. single strands or coiled-coil double-strand structures) to obtain the best superposition of atoms involved in interchain hydrogen bonding. Owing to the potential conformational flexibility of antiparallel structures, initial approximations of individual antiparallel strand conformational geometry were derived by least-squares fits of individual regular model conformations to observed structural co-ordinates. These conformations were subsequently systematically modified in order to obtain the best overall fit to the observed structure that minimized the deviations from ideality in the interchain hydrogen bonds.

Protein co-ordinate data were obtained from the Brookhaven Protein Data Bank (Bernstein *et al.*, 1977) and the Atlas of Macromolecular Structure on Microfiche (Feldman, 1976). Several structures from this atlas are reproduced or referred to here and are designated by S (Sheet) or B (Barrel), followed by fiche number, row and column. Reference to this source will provide specific residue numbering and inclusive references to the respective structure determinations.

3. Results

(a) *Conformational properties of regular antiparallel structures*

(i) *Flat antiparallel structures*

Figure 1 shows a "classical" flat antiparallel β-sheet having straight 2·8 Å NHO hydrogen bonds (Pauling & Corey, 1951). The structure shown is the unique solution having straight (NOC′) hydrogen bonds and lies on the $n = 2$ line of the ϕ, ψ plot at $\phi = -147°$, $\psi = 145°$ (Fig. 2). Owing to the antiparallel N to C sense of the chains, the arrangement possesses local dyad symmetry elements perpendicular to the plane of the sheet that are centrally located in each of the "large" and "small" hydrogen-bonded rings of the structure (Fig. 1). The presence of the dyad elements allows the continuous deformation of the structure concomitant with the symmetrical bending of the hydrogen bonds at the carbonyl oxygen in the plane of the oxygen sp^2 orbital. As described by Hagler *et al.* (1974), this bending corresponds to an isoenergetic deformation mode of the amide hydrogen bond. As a consequence of this added degree of freedom, there exists a continuously defined set of *flat* antiparallel structures whose ϕ, ψ values are uniquely correlated with a given hydrogen bond geometry (Fig. 2). As shown in Figure 3, all such structures retain essentially perfect interchain hydrogen bonds. Analysis of the correlated flat sheet ϕ, ψ behavior that accompanies this deformation suggests that the straight hydrogen bond structure ($\delta = <$ C–O–N $= 180°$) is an extended limit for the flat

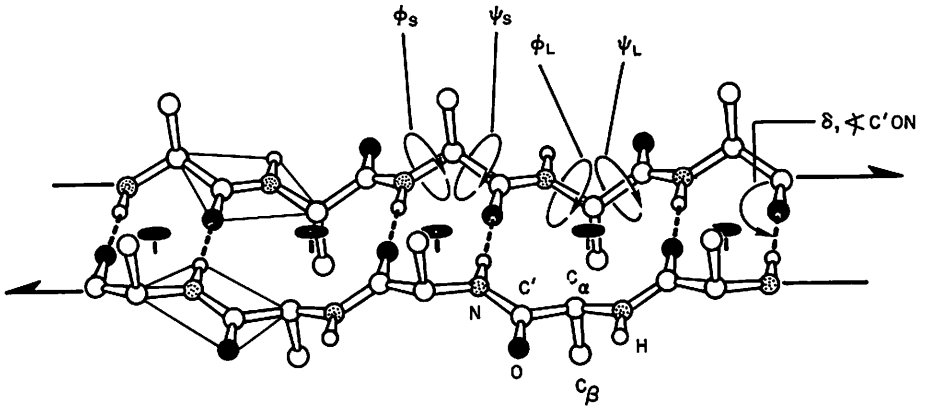

FIG. 1. A schematic illustration of a section of flat antiparallel β-sheet. The structure is composed of individual 2-fold helical chains that are arranged with opposite N to C polypeptide chain sense. Owing to the antiparallel arrangement of the chains in the structure, there are additional 2-fold rotational symmetry axes centrally located in each of the large and small hydrogen-bonded rings perpendicular to the plane of the sheet. The low-energy degrees of conformational freedom in the structure are the backbone torsional angles in the small (ϕ_S, ψ_S) and large (ϕ_L, ψ_L) hydrogen-bonded rings of the structure, and the C'ON hydrogen-bond angle (δ).

parallel structure and that the optimal preservation of the interchain hydrogen bonds is maintained only when the hydrogen bonds of the small ring buckle in an outward direction (defined as $\delta < 180°$). In contrast to the flat parallel structure where the interchain Cβ contact distances are equivalent, the Cβ contact distances for the classical flat antiparallel sheet ($\delta = 180°$) appreciably differ for the large (3·7 Å) and small (5·7 Å) hydrogen-bonded rings of the structure. The large ring Cβ contact is slightly less than the nominal 4 Å minimum contact distance for interacting methyl groups (Dickerson & Geis, 1969). However, as δ becomes more acute and the repeat period of the structure shortens, both the small and large ring Cβ interaction distances change (Fig. 4), so that at $\delta = 171°$, $\phi = -134°$, $\psi = 131°$, they are equivalent at 4·8 Å. Further shortening of the structure eventually results in the steric interaction of the small ring Cβ methyl groups at $\delta = 163°$, $\phi = -125°$, $\psi = 122°$, so defining a second limit for sterically acceptable flat structures.

(ii) *Antiparallel twisted conformations*

Following the treatment of the parallel sheets, there are two different symmetrical twisting deformations of the antiparallel sheet that correspond to structures having polypeptide chains of straight helical (all ϕ and ψ values identical) or coiled-coil (dipeptide repeating unit) conformation.

(iii) *Regular coiled-coil antiparallel structures*

As shown in Figure 1, any twisting deformation of the double-strand structure that preserves the interchain hydrogen bonds must preserve the local dyad

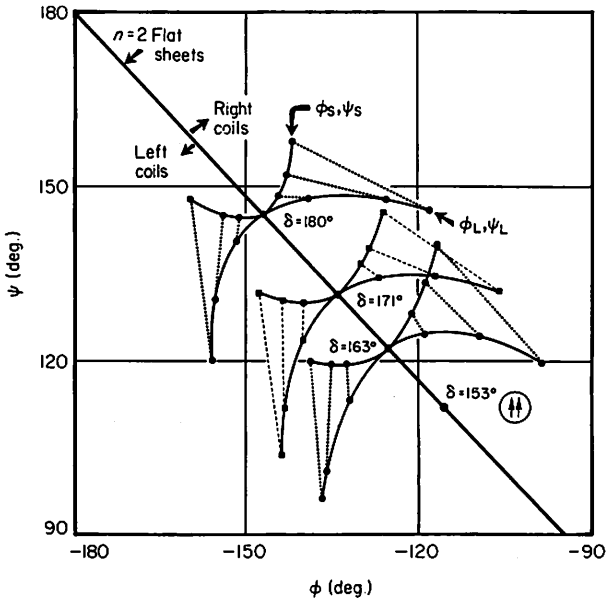

FIG. 2. A ϕ, ψ plot showing the conformational behavior for flat and coiled-coil, double-strand, twisted arrangements of antiparallel β-sheets of variable hydrogen-bond geometry (δ). Flat structures with symmetrically bent hydrogen bonds form a continuous set of conformations that lie on the $n = 2$ line. As the NOC' hydrogen-bond angle δ becomes progressively more acute, the ϕ, ψ values for the corresponding flat structures become progressively more similar to the conformation of the parallel flat sheet, which occurs at $\phi = -116°$, $\psi = 112°$. The geometry of some representative flat structures are shown in Fig. 3. As shown in Fig. 4, the accessible range of δ is restricted by interchain Cβ contact interactions. When isolated double-strand structures are twisted, the interchain hydrogen bond geometry is preserved when the local dyad axes of both large and small hydrogen-bonded rings of the structure are also preserved. The resulting twisted structures are composed of coiled-coil polypeptide chains with a dipeptide repeating unit. This twisting deformation is continuous and results in different conformations for residues in the small and large rings of the twisted structures. Note, however, that the local conformations corresponding to a given coiled-coil twisted configuration are correlated; i.e. there exists a conformationally unique pathway for the co-operative coiled-coil twisting of an isolated double-strand structure that best preserves the interchain hydrogen bonding for every value of δ. Broken or dotted lines connecting points on the continuous curves show how the conformational behavior in the small rings (ϕ_S, ψ_S) correlates with that in the large rings (ϕ_L, ψ_L). Coiled-coil antiparallel sheet geometry is shown in Fig. 5. The curves shown are representative; similar curves are obtained for any (variable δ) starting flat structure.

symmetry of both the large and small hydrogen-bonded rings. This in turn requires that the local conformations about the α-carbons on opposite sides of each hydrogen-bonded ring be identical. However, it is clear that the conformational behavior of residues situated in the large and small hydrogen-bonded rings of the structure must be different since, if they were the same, the resulting structure would be composed of straight-helical twisted chains that would eventually diverge spatially. Twisting of an isolated double-strand antiparallel sheet will therefore result in coiled-coil structures whose polypeptide chains have equivalent values of ϕ_S, ψ_S, for all small rings, and ϕ_L, ψ_L for all large rings. Although there exists an infinite number of possible coiled-coil conformations characterized by a dipeptide repeating unit (Nishikawa & Scheraga, 1976), the mechanical coupling of the large

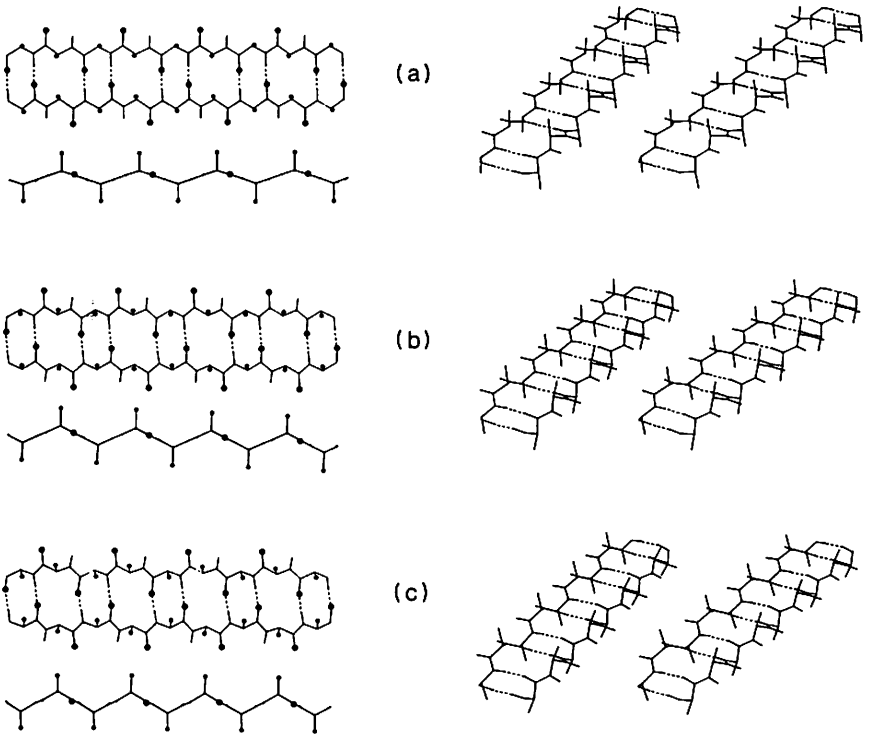

FIG. 3. Representative flat antiparallel β-sheets with variable hydrogen bond (NOC′) angle. (a) Classical structure with straight interchain hydrogen bonds, $\phi = -147°$, $\psi = 145°$, $\delta = 180°$. (b) Structure with $\delta = 171°$, $\phi = -134°$, $\psi = 131°$. This structure has equivalent Cβ spacings in both large and small rings. (c) Structure with $\delta = 163°$, $\phi = -125°$, $\psi = 122°$. Side-chain Cβ and carbonyl oxygen atoms are dotted (small and large, respectively) in side and plan views. Geometrical data are given in Fig. 4. Note that all structures preserve exact dyad symmetry in both large and small hydrogen-bonded rings.

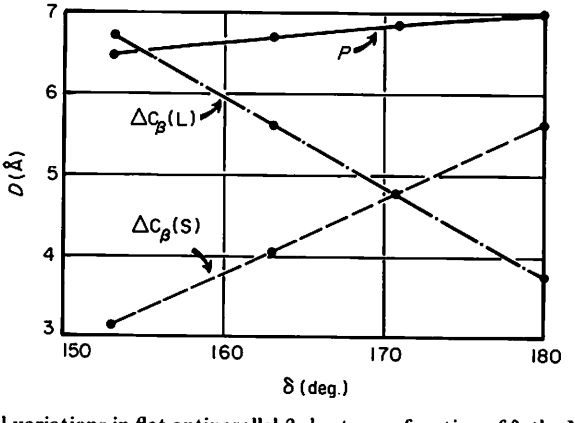

FIG. 4. Geometrical variations in flat antiparallel β-sheets as a function of δ, the NOC′ hydrogen-bond bend angle. P is the dipeptide repeat period, $\Delta C\beta(L)$ is the cross ring Cβ contact distance in the large hydrogen-bonded ring of the flat structure, and $\Delta C\beta(S)$ is the contact distance across the small rings.

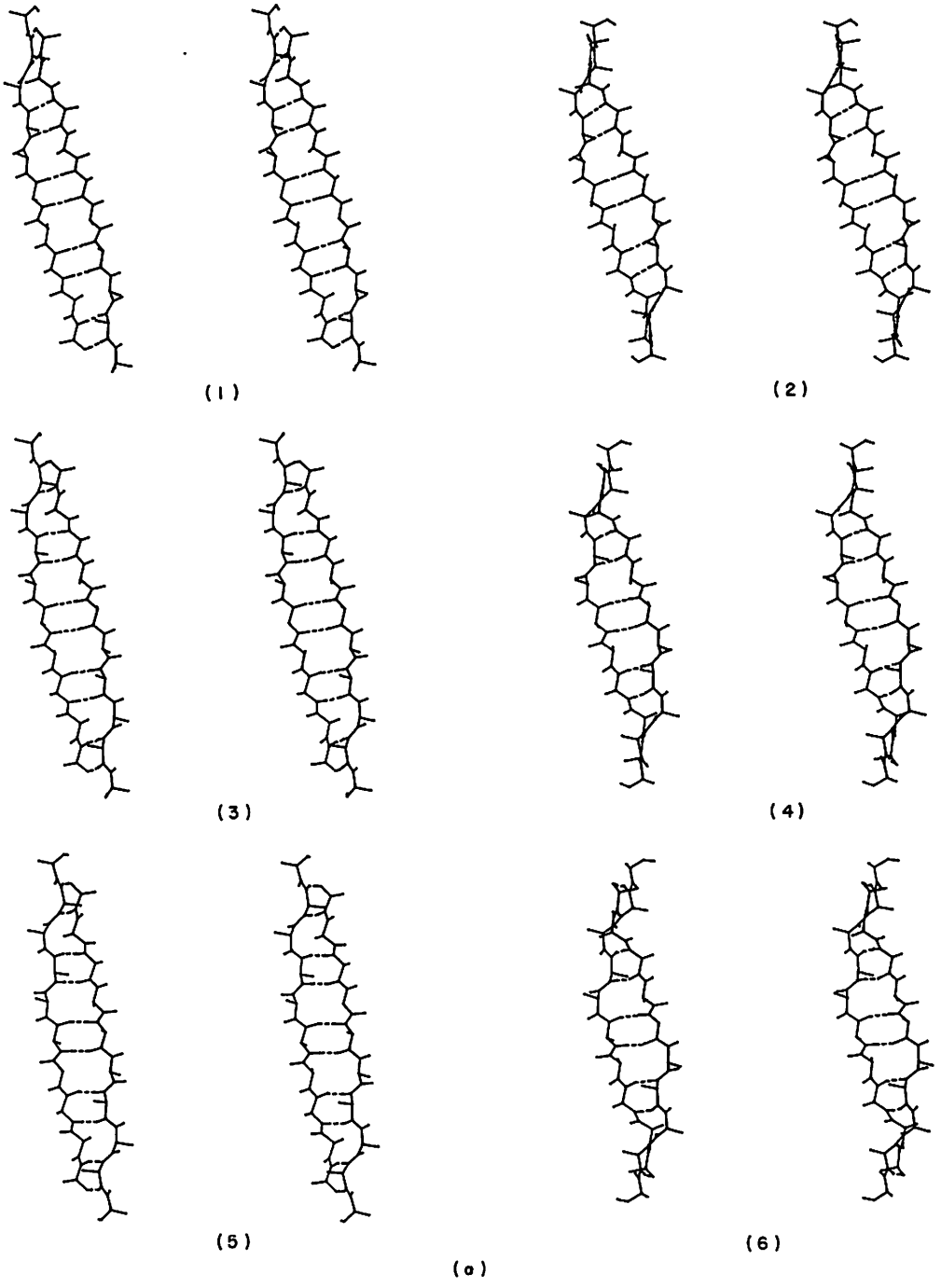

FIG. 5. Representative right coiled, double-strand antiparallel coiled-coil β-sheets. (a) Stereoscopic views of the structures; (b) corresponding projection views down the superhelical axes of the structures. (1) Structure with $\delta = 180°$, $\phi_S = -142°$, $\psi_S = 152°$, $\phi_L = -126°$, $\psi_L = 148°$. (2) Structure with $\delta = 180°$, $\phi_S = -142°$, $\psi_S = 158°$, $\phi_L = -118°$, $\psi_L = 146°$. (3) Structure with $\delta = 171°$, $\phi_S = -128°$, $\psi_S = 140°$, $\phi_L = -116°$, $\psi_L = 134°$. (4) Structure with $\delta = 171°$, $\phi_S = -126°$, $\psi_S = 146°$, $\phi_L = -106°$, $\psi_L = 132°$. (5) Structure with $\delta = 163°$, $\phi_S = -119°$, $\psi_S = 134°$, $\phi_L = -109°$, $\psi_L = 128°$. (6) Structure with $\delta = 163°$,

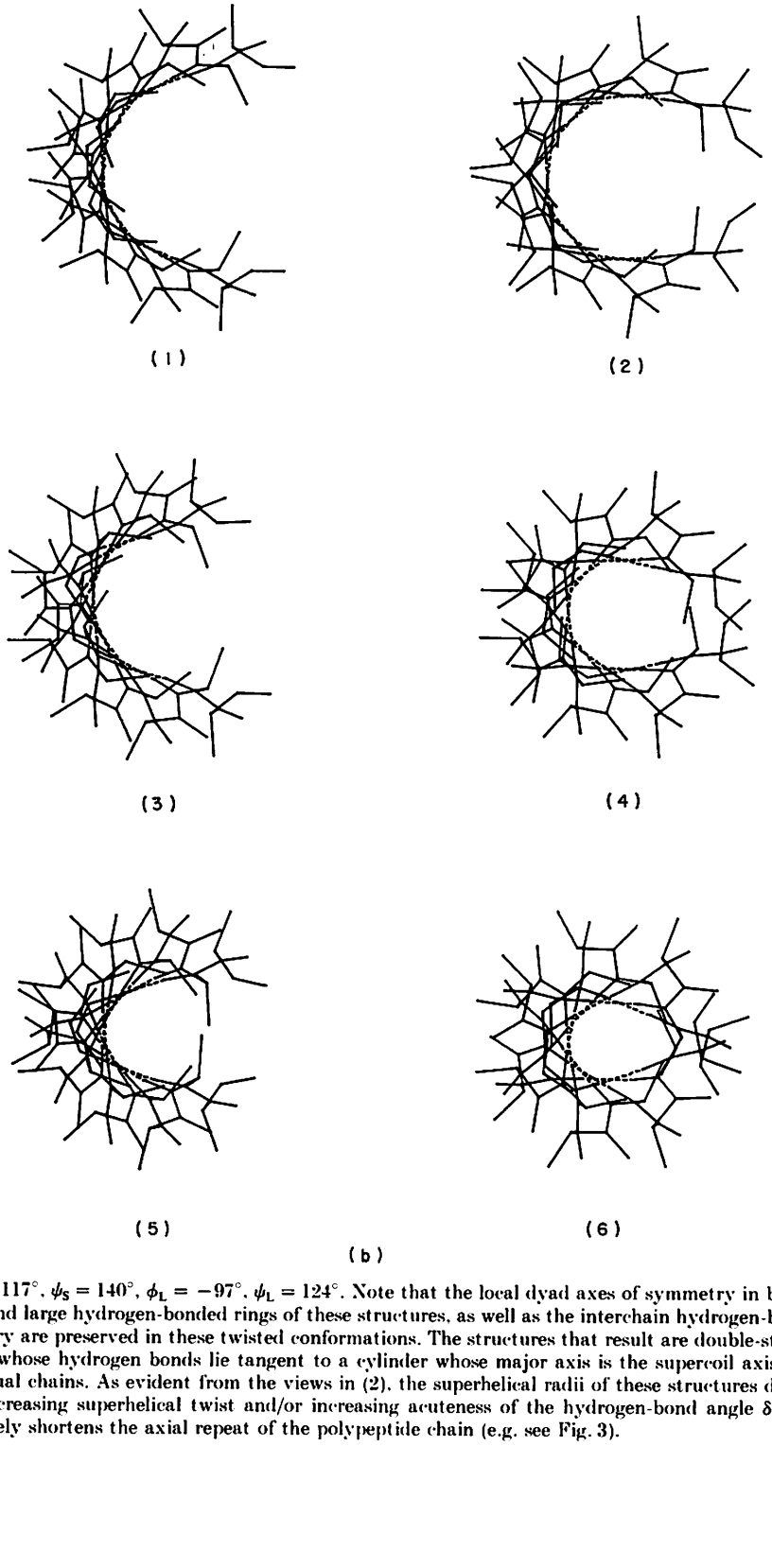

(b)

$\phi_S = -117°$, $\psi_S = 140°$, $\phi_L = -97°$, $\psi_L = 124°$. Note that the local dyad axes of symmetry in both the small and large hydrogen-bonded rings of these structures, as well as the interchain hydrogen-bonding geometry are preserved in these twisted conformations. The structures that result are double-stranded helices whose hydrogen bonds lie tangent to a cylinder whose major axis is the supercoil axis of the individual chains. As evident from the views in (2), the superhelical radii of these structures decrease with increasing superhelical twist and/or increasing acuteness of the hydrogen-bond angle δ, which effectively shortens the axial repeat of the polypeptide chain (e.g. see Fig. 3).

and small rings in the antiparallel β-sheets gives rise to correlated conformational behavior in the twisted structure. That is to say, each twisted conformation having a specified hydrogen-bond geometry will be uniquely associated with a pair of large and small ring local conformations. This conformationally correlated coiled-coil twisting behavior is shown in Figure 2 for $\delta = 180°$, 171° and 163° hydrogen bond configurations. As shown in Figure 5, antiparallel coiled-coils form double-helical structures whose hydrogen bonds lie tangent to a cylindrical surface whose major axis is the superhelix axis of the structure as a whole. Further, as is apparent in the perfect retention of the local dyad axes of symmetry in the large and small rings, the hydrogen bonds of these structures are correspondingly regular. Consequently, insofar as hydrogen bonding is concerned, all coiled-coil antiparallel structures showing the *correlated* ϕ, ψ behavior typical of the representative geometries shown in Figure 5 are essentially isoenergetic.

(iv) *Crossing antiparallel structures*

The formation of twisted structures composed of straight helical chains (all ϕ, ψ conformational angles identical) will necessarily involve the introduction of interchain hydrogen bond irregularity between the chains, since it is evident that the chain axes must eventually diverge in space (e.g. see Fig. 10(a)).

However, in contrast to parallel structures (Salemme & Weatherford, 1981), there do not exist uniquely defined pathways associated with the optimal preservation of the interchain hydrogen bonds for the twisting of antiparallel structures composed of straight helical chains. That is to say, any flat antiparallel structure having a specified interchain hydrogen-bond geometry will, when twisted to form a crossing structure composed of straight helical chains, involve the introduction of distortions into the interchain hydrogen bonds, the extent of which is related solely to the degree of resulting interchain twist. As shown in Figure 5, the lines of constant interchain twist lie approximately parallel to the $n = 2$ line in the extended polypeptide chain region of ϕ, ψ space, so that the extent of cumulative interchain hydrogen-bond distortion is dependent only on the extent of excursion from the $n = 2$ line, independent of the interchain hydrogen-bond geometry. This situation occurs principally because the isoenergetic deformations of the hydrogen bond involve bond bending in the planes of the peptide groups of the sheet. These isoenergetic deformations consequently provide no useful degrees of freedom that can potentially improve the hydrogen bonding between straight helical, twisted polypeptide chains (e.g. see Fig. 8). However, as pointed out above, variations of the interchain hydrogen-bond geometry are accompanied by substantial variations in the cross-ring Cβ contact distances in the large and small rings of the antiparallel structures. As a consequence of this situation, antiparallel crossing conformations may to some extent be differentiated on the basis of the relative equivalence of the side-chain steric interactions, as is consistent with the assumption of most uniform packing among the side-chains of the sheet as a whole. Figure 6 shows the variation in the *difference* between large and small cross-ring Cβ contact distances for crossing antiparallel structures, from which it is apparent that the requirements for equivalent and/or sterically acceptable side-chain packing

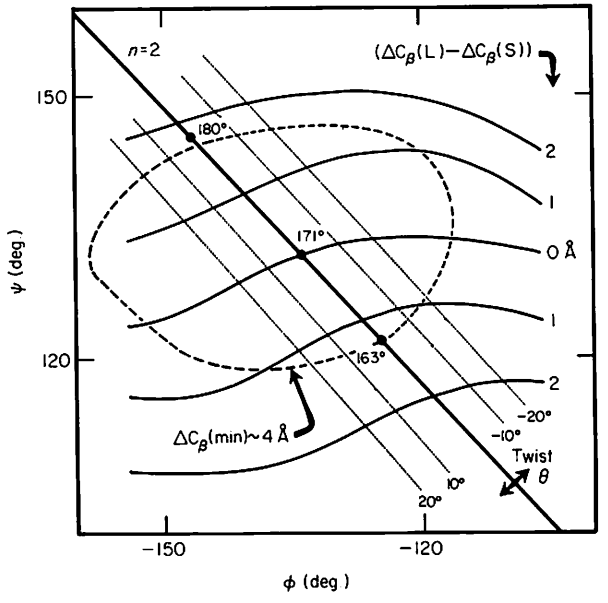

FIG. 6. A ϕ, ψ plot illustrating the behavior of twisted antiparallel β-sheets composed of straight helical (all ϕ, ψ values identical) crossing polypeptide chains. Lines of constant interchain twist (θ) run parallel to the $n = 2$ flat helical line in the plot. The roughly sigmoid curves plot the value (Å) of the difference between Cβ contact distances in the large and small rings of the various crossing chain twisted structures. Although all similarly twisted crossing structures have similar extents of cumulative hydrogen-bond distortion for an equivalent number of interchain hydrogen bonds (Fig. 8), irrespective of interchain hydrogen-bond geometry (δ), the accessible region for such structures is constrained owing to the requirements for maximally isotropic side-chain packing interactions. Structures having the most equivalent large and small cross-ring interactions lie along the curve ($\Delta C\beta(L) - \Delta C\beta(S) = 0$), which intersects the $n = 2$ line at the ϕ, ψ value corresponding to an interchain hydrogen-bond geometry with $\delta = 171°$. The broken contour on the plot gives the approximate limit for crossing conformations for which one or the other cross ring Cβ contacts becomes less than approximately 4 Å, a nominal value for the steric interaction of side-chain methyl groups.

interactions may serve to restrict the number of accessible conformations that otherwise have similarly distorted hydrogen bonded interactions. Figure 7 shows views of a representative regular, twisted antiparallel sheet having optimally equivalent side-chain interactions, and Figure 8 shows the hydrogen bonding behavior for equivalently packed structures as a function of polypeptide chain length and interchain twist.

(b) *Extended geometry of antiparallel β-sheets and structural comparison of model and observed structures*

The spatial configurations of antiparallel β-sheets would be expected to exhibit qualitatively similar dependencies on the nature and extent of adjacent chain hydrogen-bonded connectivity, as is observed in parallel sheet structures. For example, isolated double-strand arrangements or polypeptide chains located at the edges of sheets, where they are relatively unconstrained by the requirements for systematic across-the-sheet hydrogen-bonded interactions, would be expected to be

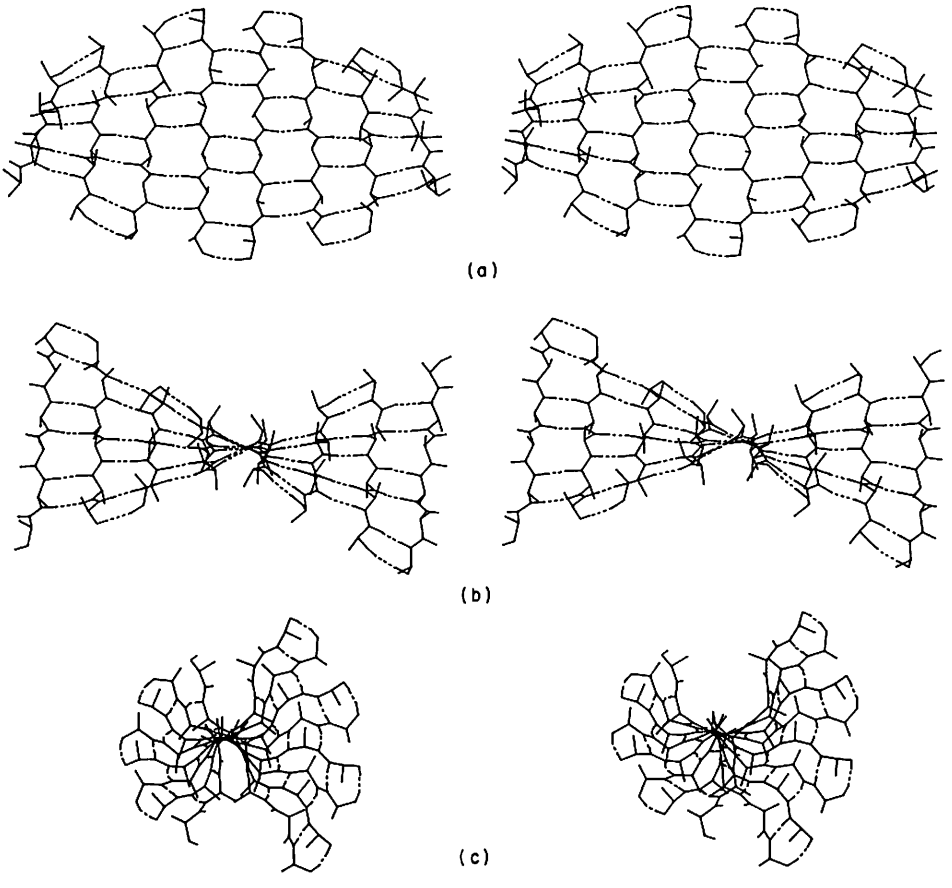

FIG. 7. A regular antiparallel twisted β-sheet composed of straight helical crossing chains. (a) View normal to the plane of the central hydrogen-bonded ring of the sheet. (b) View down the central chain axes. (c) Edge view. The structure is composed of chains with $\phi = -122°$, $\psi = 135°$ and $\delta = 171°$. Average hydrogen bond length is 2·77 Å with a standard deviation of 0·30 Å. Interchain twist as defined in Fig. 8 is 26·7°.

best approximated as coiled-coil conformations. Likewise, multiple-strand sheets having extensive across-the-sheet hydrogen-bonded interactions might be expected to be best approximated as arrays of straight helical chains, since these conformations are optimally extensible into multiple-strand structures with equivalent interchain interactions. However, it is clear from the preceding description of the properties of regular coiled-coil and straight-helical chain antiparallel β-sheets that, owing to the potential variability of the interchain hydrogen-bond geometry, antiparallel sheets possess a considerable degree of conformational flexibility that is not present in parallel sheets.

This property endows antiparallel sheets with a considerable degree of elasticity, so that their extended spatial geometries are strongly influenced by both localized and long-range packing effects. In what follows, we show how these effects, in concert with the geometrical constraints imposed by the requirements for the

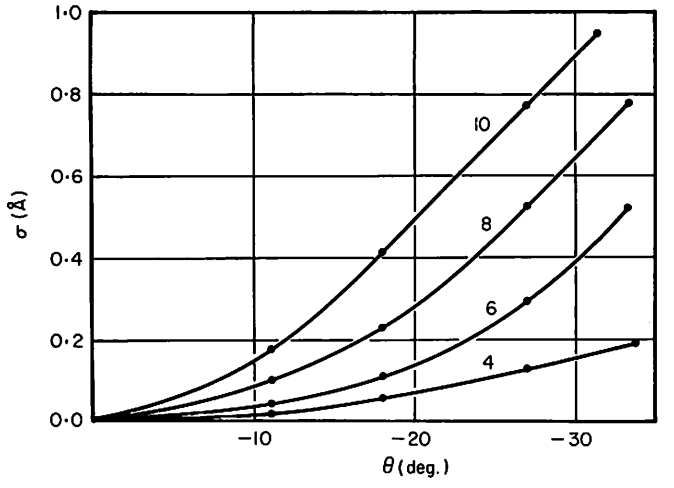

FIG. 8. A plot showing the variation in the standard deviation in hydrogen bond length (σ) as a function of interchain twist (the angle between vectors C$\alpha(i)$ and C$\alpha(i+2)$ for adjacent chains) for antiparallel crossing structures with a variable number of interchain hydrogen bonds. The curves shown were computed for crossing chains with $\delta = 171°$, along the equivalent cross ring Cβ contact line shown in Fig. 6. The behavior shown in essentially identical for other interchain hydrogen-bond geometries.

preservation of interchain hydrogen bonding, manifest themselves in some known protein structures.

(i) *Double-strand sheets*

Isolated, double-strand antiparallel sheets occur frequently in proteins of known structure. Almost invariably these regions are observed to form coiled-coil conformations similar to those shown in Figure 5. Figure 9(a) shows a representative least-squares superposition of a regular model structure with the antiparallel β-coil in pancreatic trypsin inhibitor (Huber *et al.*, 1972). The mean superposition error for the α-carbons of the model and observed structures is 0·52 Å. As shown in Figure 9(b), this strongly twisted configuration gives rise to an intimately close-packed arrangement of the polypeptide side-chains. The structure as a whole consequently appears to be both twisted (in response to the minimization of the backbone conformational potential) and axially compressed (with the accompanying introduction of non-linearity into the interchain hydrogen bonds: cf. Fig. 5) to the maximum possible extent consistent with the steric limitations of side-chain packing, to yield a structure that is overall tightly packed. Additional examples of this arrangement which, as shown below, also occur in more extended sheets, may be seen in thermolysin (AMSOM S2B14: Feldman, 1976) and lactate dehydrogenase (AMSOM S2C13: Feldman, 1976).

(ii) *Triple-strand sheets, helicoid surfaces and β-bulges*

Figure 10 schematically summarizes the geometrical properties of triple-strand antiparallel structures. Part (a) shows the geometry of a structure composed of

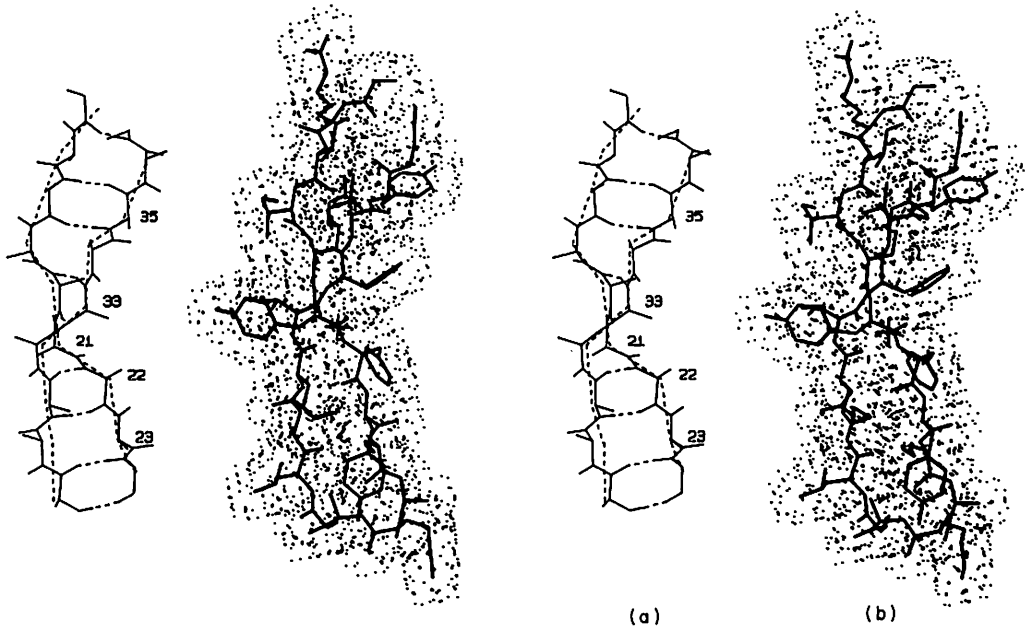

FIG. 9. (a) A least-squares superposition of a regular antiparallel coiled-coil with $\phi_S = -114°$, $\psi_S = 150°$, $\phi_L = -92°$, $\psi_L = 114°$, $\delta = 163°$ (unbroken lines) with the α-carbon positions of the double-strand β-sheet (broken lines) in pancreatic trypsin inhibitor. The average superposition error in model *versus* observed Cα co-ordinates is 0·52 Å. Average model hydrogen bond length (N–O) is 2·79 Å with a standard deviation of 0·13 Å.

(b) A pseudo-space-filling representation of the trypsin inhibitor β-coil illustrating the intimate side-chain packing attained in this strongly twisted conformation.

identical, straight-helical chains in which the interchain hydrogen bonds become progressively longer toward the ends of the chains. However, since the polypeptide chain period of the antiparallel structure can vary concomitant with variations in the interchain hydrogen-bond geometry, the arrangement shown in part (a) can deform spontaneously to give the structure of helical symmetry shown in part (b). The resulting helicoid surface structure has overall equivalent hydrogen-bonding geometry, as well as more nearly equivalent overall packing interactions on both sides of the sheet. It is composed of a straight-helical central chain, about which are wound exterior chains of coiled-coil conformations. (We emphasize that the coiled-coil conformations that characterize such structures are not necessarily identical to those conformations characterizing the twisting behavior of *isolated* double-strand antiparallel sheets, since the operative geometrical constraints corresponding to the optimal overall preservation of interchain hydrogen bonding will differ, depending on the actual hydrogen bond plan of the sheet.) Since the exterior coiled-coil chains lie on a cylindrical surface whose axis is defined by the central chain, it is clear that the exterior chains must generally traverse a longer pathlength than the corresponding chains in a structure composed wholly of straight-helical chains. For structures of moderate twist, this situation is easily achieved, since both the central and exterior chains can suitably alter their local conformations to give an overall

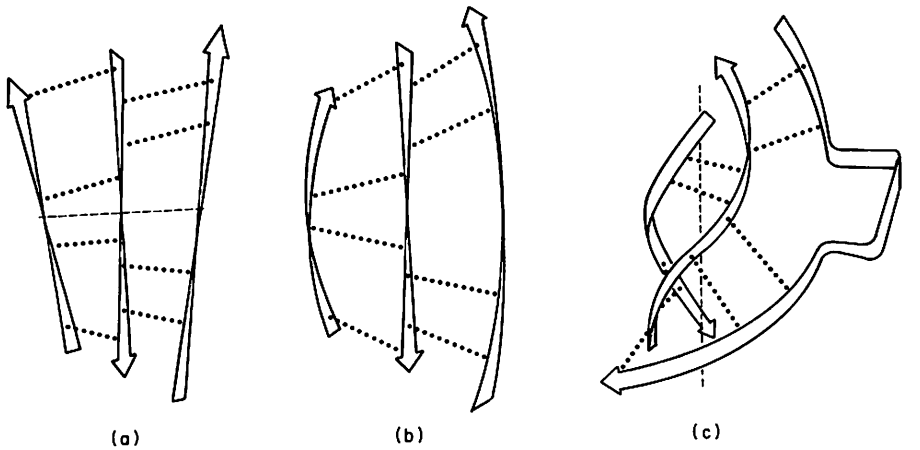

FIG. 10. Schematic illustration of the properties of triple-strand antiparallel β-sheets. (a) An arrangement of 3 straight-helical crossing chains. Since the chains of the structure are straight, they diverge towards the ends of the sheet where the interchain hydrogen bonds must necessarily be somewhat longer than in the center of the sheet (i.e. along the broken line). (b) Since antiparallel chains can have variable repeat periods concomitant with accompanying variations in interchain hydrogen-bond geometry, the structure shown in (a) can readily deform into an arrangement where the central strand remains a straight helix, but the outer strands become more extended and take on coiled-coil conformations. These edge chains now lie on the surface of a cylinder, whose major axis is coincident with the central straight helical chain, so that the hydrogen bonds are of equal length along the cylinder axis. (c) In situations where 2 adjacent strands of the sheet take on strongly twisted coiled-coil character, the 3rd exterior strand can no longer become sufficiently extended to regularly satisfy the geometrical requirements of interchain hydrogen bonding, since it must lie on a cylindrical surface having the same super-coil axis (broken line) as the strongly twisted coiled-coil chains. As a consequence, such arrangements typically compensate for this effect by the incorporation of extra "bulge" residues in the exterior strand. In observed protein structures, there appears to exist a practically continuous distribution of structures having geometries more or less representative of the arrangement shown in (b) where the hydrogen bonding and packing interaction are overall maximally equivalent, and (c) where the particularly good packing interactions in the strongly twisted coiled-coil dominate the spatial behavior of the structure.

geometry that is consistent with the optimal preservation of the interchain hydrogen bonding throughout the sheet. Figure 11(a) and (b) shows views of a representative regular model structure, and Figure 11(c) shows model *versus* observed superposition of a region in ribonuclease A (Bernstein *et al.*, 1977). The triple-strand antiparallel helicoid arrangement appears frequently in proteins of known structure (see e.g. AMSOM S41i4, S2M11 and S4K10; Feldman, 1976), as well as mixed parallel–antiparallel structures (see Fig. 16(d)).

Figure 10(c) shows an alternative triple-strand arrangement frequently observed in antiparallel β-sheets, which occurs when the particularly good localized packing interactions are attained by two adjacent strands. In this case, the well-packed strands tend to conform to strongly twisted coiled-coil configurations similar to those characterizing isolated double-strand sheets. This requires that the remaining strand be a coiled-coil that also conforms to the superhelix axis defined by the first two strands, but which must consequently have a longer polypeptide repeat period than the double-strand coiled-coil chains since it lies on a cylindrical surface of large effective radius. Since there are limits to the accessible conformations that

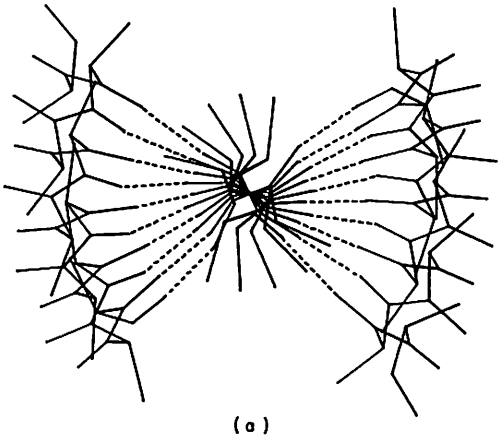

(a)

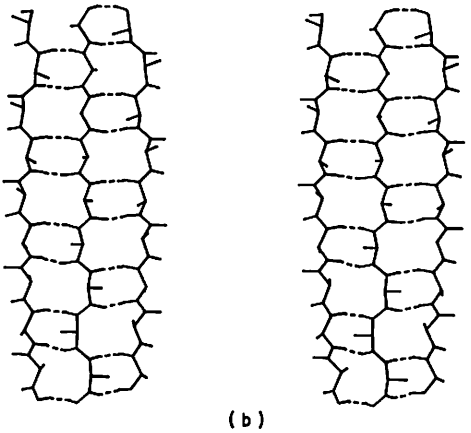

(b)

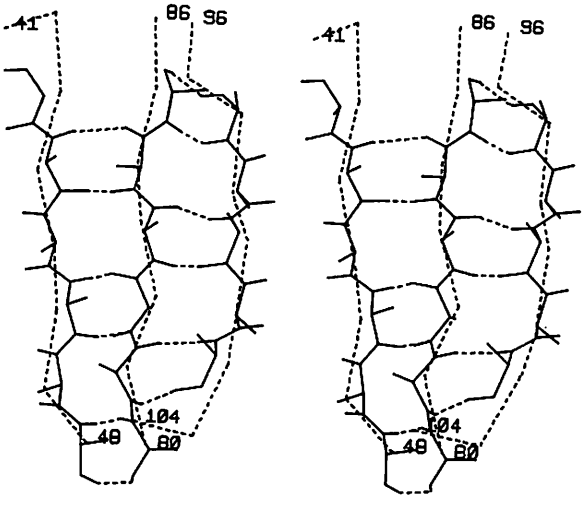

(c)

FIG. 11.

can accommodate the extended period, superhelical twist and hydrogen-bonding geometric requirements required by the addition of a third outer strand to a highly twisted antiparallel coiled-coil, such arrangements necessitate the introduction of a conformational defect in the outer strand. Typically, this defect takes the form of an extra residue inserted into the exterior chain, thus forming what Richardson and co-workers have termed a β-bulge (Richardson *et al.*, 1978).

(iii) *Multiple-strand sheets*

As evident from the preceding description of triple-strand antiparallel sheets, extended antiparallel arrays can manifest a variety of spatial geometries that basically reflect different ways in which local or extended side-chain packing forces interact with the the conformational requirements associated with the maintenance of interchain hydrogen bonding. For this reason few, if any, of the observed multiple-strand antiparallel β-sheets exhibit extended spatial geometries characteristic of regular crossing chain structures.

Figure 12(a), for example, shows the four most regularly hydrogen-bonded strands of the dimer–interface antiparallel sheet in concanavalin A (Hardman & Ainsworth, 1972; Reeke *et al.*, 1975). Although this sheet is reasonably well-approximated as a nearly flat straight-helical chain structure, more detailed examination showed that the optimal model *versus* observed α-carbon superposition (average superposition error 0·72 Å) was obtained when individual strands of the structure were separately approximated as conformationally differing, but regular, straight-helical chains. The best subsequent optimization of both Cα fits and interchain hydrogen bonds results in a model having one strand of slight left-handed twist. The incorporation of this strand tends to untwist the sheet. The probable origin of this effect lies in the fact that this sheet forms part of a large extended sheet in the dimer aggregate that is bent across the dimer dyad axis owing to extended packing interactions between the monomer subunits (Fig. 12(b)).

Figure 13 shows views illustrating some examples of continuously deformed sheets having apparent concave curvature. The spatial conformation attained by such sheets reflects the fact that, owing to the relatively large extent of conformational flexibility in antiparallel sheets, they can form extended arrays of strands having essentially continuously varying, slight coiled-coil character. Since

---

FIG. 11. (a) Axial projection and (b) stereoscopic views of a triple-strand antiparallel β-sheet with a straight helical central chain ($\phi = -113°$, $\psi = 112°$) and coiled-coil exterior chains ($\phi_1 = -127°$, $\psi_1 = 124°$, $\phi_2 = -113°$, $\psi_2 = 130°$). Average N–O hydrogen bond length with $\delta = 163°$ is 2·78 Å, standard deviation 0·14 Å. (c) A least-squares superposition of an extended triple-strand region of a larger β-sheet in ribonuclease A (broken lines) with a regular model structure. The model structure is composed of a straight helical central chain ($\phi = -102°$, $\psi = 131°$) and conformationally differing regular exterior coiled-coil chains; residues 43 to 48, $\phi_1 = -102°$, $\psi_1 = 128°$, $\phi_2 = -116°$, $\psi_2 = 134°$, residues 98 to 102, $\phi_1 = -134°$, $\psi_1 = 118°$, $\phi_2 = -102°$, $\psi_2 = 128°$. The conformations of the exterior chains appear to differ owing to different extended hydrogen bonding and packing interactions at the edges of the sheet. The extended model structure was generated by least-squares superposition of atoms involved in the interchain hydrogen bonds as described in Methods. The resulting model gives an average error of fit of 0·56 Å with the observed structure for corresponding α-carbons. The average hydrogen bond length in the model is 2·72 Å with a standard deviation of 0·29 Å.

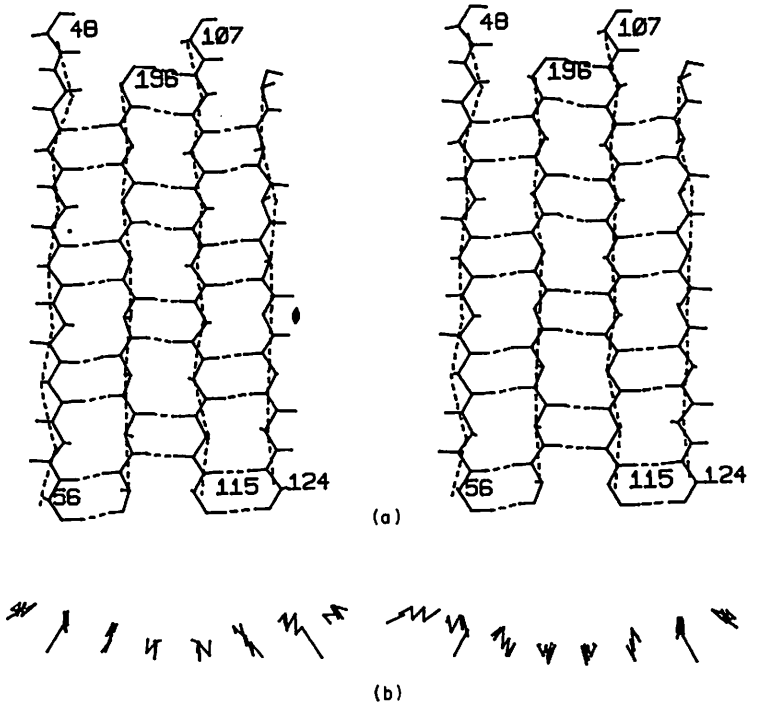

FIG. 12. (a) A least-squares fit of a model composed of regular straight helical polypeptide chains superimposed on the 4 most regular strands of the dimer interface β-sheet in concanavalin A (Bernstein *et al.*, 1977, File 2CNA, dashed connected α-carbon positions). The model is composed of straight helical chains of differing conformations: i.e. residues 48 to 56 are approximated as a chain with $\phi = -150°$, $\psi = 152°$, residues 189 to 196 with $\phi = -152°$, $\psi = 146°$, residues 107 to 115 with $\phi = -142°$, $\psi = 142°$, and residues 124 to 131 with $\phi = -152°$, $\psi = 152°$. Least-squares fitting of the hydrogen-bonded interactions between these chains produces an extended model whose corresponding α-carbons fit the observed structure with an average error of 0·72 Å, with hydrogen bonds of 2·82 Å length and 0·31 Å standard deviation. (b) A projection of the observed co-ordinates of the dimer sheet perpendicular to the dimer dyad axis. Note that the sheet is bent along a line parallel to the chain directions and approximately perpendicular to the dyad axis. This deformation appears to untwist the sheet, residues 189 to 196 of the model consequently being best approximated as a straight helical chain of slight left-handed superhelical twist (i.e. lying to the left of the $n = 2$ line).

hydrogen-bonded antiparallel coiled-coil arrays in general form structures that conform to cylindrical surfaces (see Fig. 5), the resulting structures appear to have a net cylindrical curvature. Figure 13(a), for example, shows views of the extended antiparallel sheet in glyceraldehyde-3-phosphate dehydrogenase (Buehner *et al.*, 1974). In this sheet, the central chains can be seen to have the characteristic conformational character of the double-strand antiparallel coiled-coil, about which are organized coiled-coil chains of more extended conformation. Figure 13(b) shows an exterior sheet region in concanavalin A. The central strands of this sheet appear to be bowed, rather than twisted. As shown in Figure 14(a), structures exhibiting this geometric behavior cannot be composed of twisted coiled-chains, but instead assume coiled-coil conformations that resemble those produced in structures whose

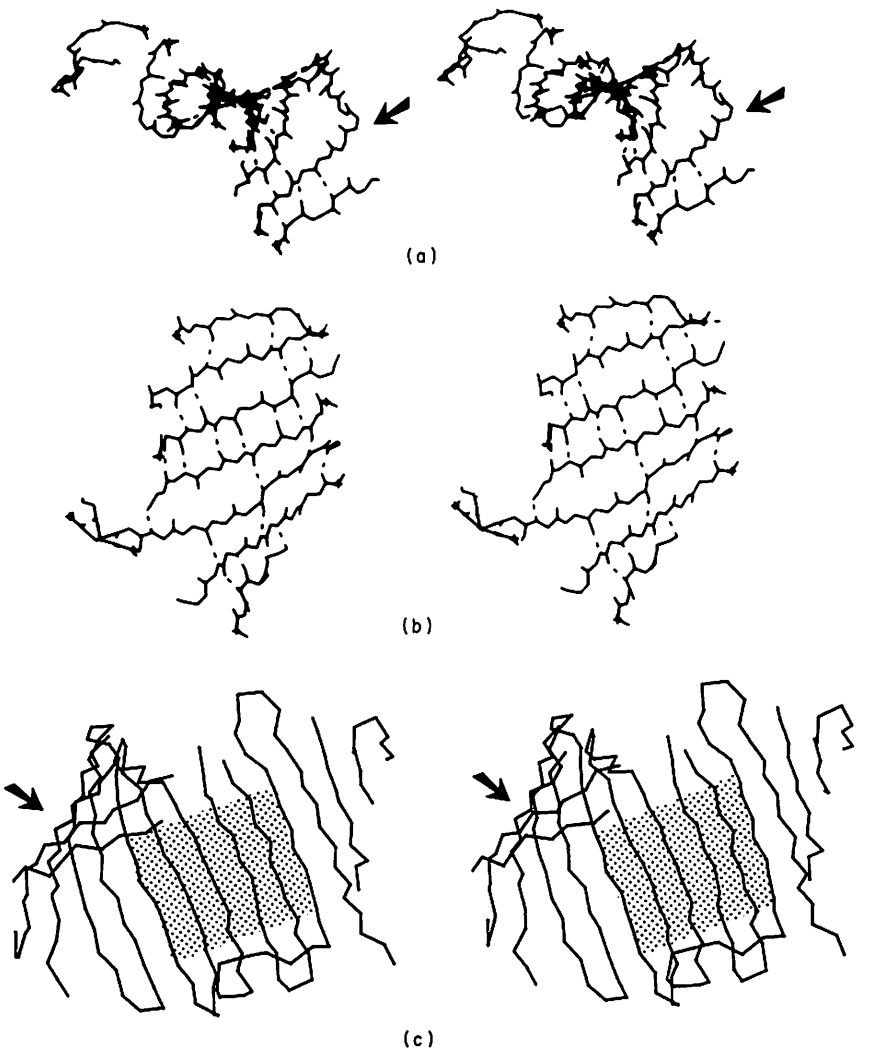

FIG. 13. Examples of continuous deformations in antiparallel β-sheets.

(a) A region of the antiparallel β-sheet in glyceraldehyde-3-phosphate dehydrogenase (AMSOM S2G15, Feldman, 1976). The central strands of this structure have slight coiled-coil character giving the overall sheet apparent cylindrical curvature. Note that one outer strand contains a bulge (arrow), presumably owing to the inability of this strand to become both sufficiently extended and maintain the geometry required for regular hydrogen bond formation to the inner coiled-coil strands (cf. Fig. 10(c)).

(b) The exterior antiparallel β-sheet in concanavalin A (AMSOM S7I1, Feldman, 1976). This sheet is composed of coiled-coiled chains that appear to have become untwisted in the central region, in response to different packing interactions on opposite sides of the sheet, which cause it two bend about a cylindrical axis at right angles to the direction of the polypeptide chains (see Fig. 14).

(c) The β-sheet in bacteriochlorophyll binding protein (Bernstein *et al.*, 1977). The shaded overlay shows the region of this sheet which, as described by Matthews *et al.* (1979), is essentially flat, presumably owing to the extensiveness of the regular hydrogen bonding both along and across the sheet in this region (see Fig. 8). The staggered region of the structure (arrow) exhibits continuous curvature that results from the structure's chains taking on slight coiled-coil character. The structures shown here manifest the continuously deformable properties inherent in extended antiparallel β-sheets. Such structures are consequently not readily modeled as arrays of conformationally identical chains.

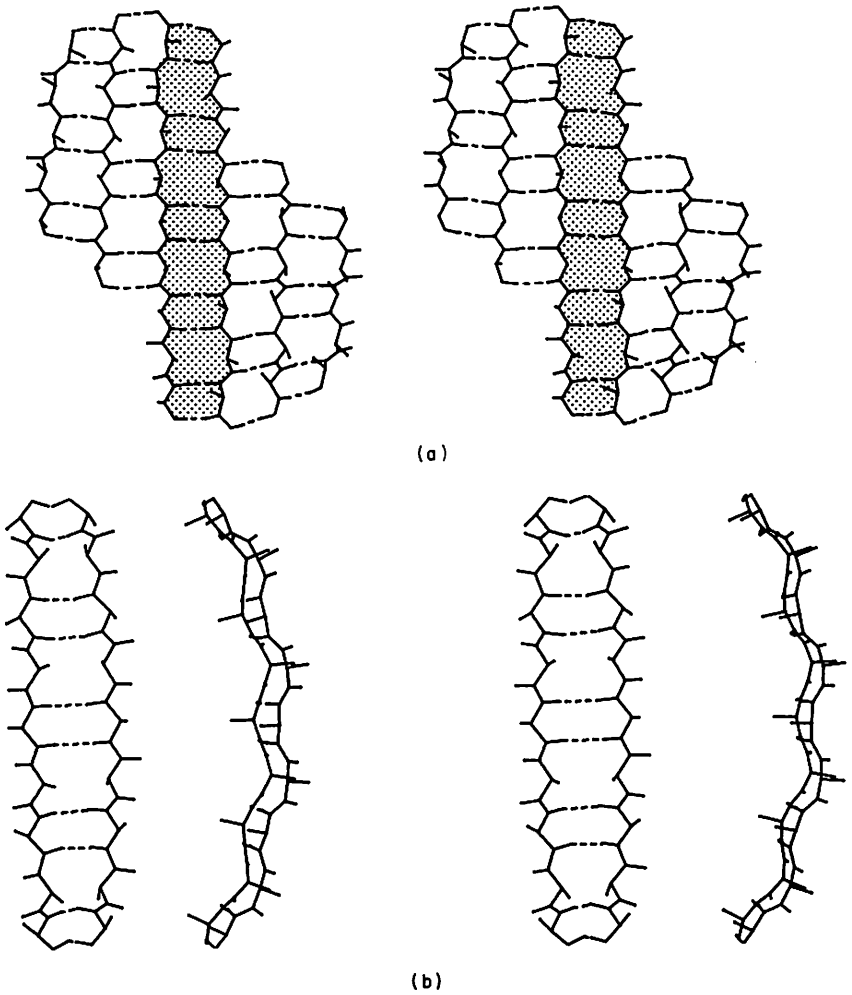

FIG. 14. (a) An extended antiparallel β-sheet composed of identical slightly twisted coiled-coil chains with $\phi_1 = -130°$, $\psi_1 = 134°$, $\phi_2 = -126°$, $\psi_2 = 134°$) with hydrogen bonds of average length 2·79 Å, standard deviation 0·24 Å. The introduction of more extensive curvature into such structures necessitates that the outer strands of such arrays assume more extended coiled-coil conformations, which will generally result in an arrangement having a continuously varying curvature (see e.g. Fig. 13(a)). (b) Some continuously deformed β-sheets exhibit sheet curvature that apparently reflects the effects of extended packing forces that tend to bend the sheet (see e.g. Fig. 13(b)). Bending the sheet so that its polypeptide chains lie on a cylindrical surface whose major axis lies perpendicular to the chain directions causes the chains to untwist and the interchain hydrogen bonding to become somewhat poorer relative to more twisted, but less bent, coiled-coil conformations. Shown are plan and side views of a conformationally regular, bent antiparallel β-sheet composed of coiled-coil chains whose alternating ϕ, ψ values lie on the flat helical $n = 2$ line of the ϕ, ψ plot ($\phi_1 = -147°$, $\psi_1 = 145°$, corresponding to the $\delta = 171°$ flat sheet, $\phi_2 = -134°$, $\psi_2 = 131°$, corresponding to the $\delta = 171°$ flat sheet conformation). Note that this structure is not twisted, but is instead continuously bent about a cylindrical surface whose major axis (which would be horizontal in the Figure) is locally perpendicular to the mean direction of the polypeptide chains. Bending the sheet in this way preserves pseudo-symmetry in the large and small hydrogen-bonded rings and is allowed owing to the period variability inherent in antiparallel sheet structures (Fig. 3). For the structure shown, the average hydrogen bond length is 2·67 Å with a standard deviation of 0·84 Å. Attempts at improving the hydrogen bonding in bent structures results either in a flattening of the sheet or the generation of a *twisted* coiled-coil (Fig. 5).

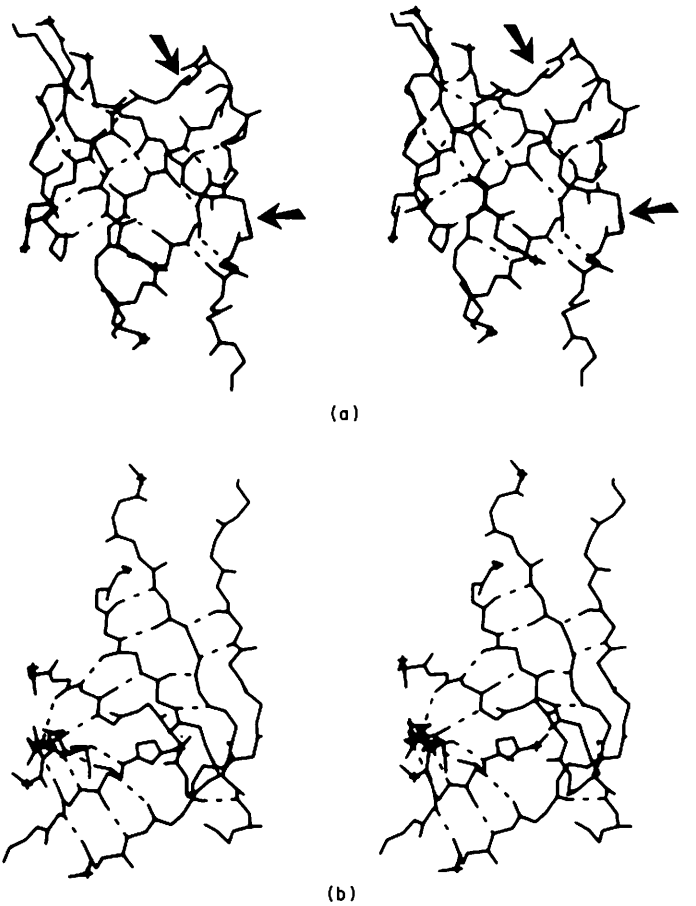

FIG. 15. The amino-terminus antiparallel β-barrel in α-chymotrypsin (Birktoft & Blow, 1972). The most extensively hydrogen-bonded regions of this structure can be viewed as locally distorted arrangements of either of the idealized triple strand structures shown in Fig. 10(b) and (c). Note that closure of the structure requires the introduction of strong localized interchain twists that produce bulges (arrows). (a) AMSOM B1E1; (b) B131. The view shown in (b) emphasizes the divergence of the chains towards the ends of the barrel, which reflects the limitations in the twist that may be accommodated in external antiparallel coiled-coil sheets.

polypeptide chains have alternate flat-helical backbone conformations (Fig. 14(b)). Figure 13(c) shows the extended antiparallel β-sheet comprising the majority of the polypeptide backbone structure in bacteriochlorophyll binding protein (Matthews *et al.*, 1979). This sheet is essentially flat in the central region where it is most extensively hydrogen-bonded across the sheet, but merges continuously into a region of coiled-coil chains that effect closure of the sheet.

Although it may appear that the antiparallel coiled-coil conformations might naturally lend themselves to the formation of regular closed barrel structures, in which all chains of the structure are contiguously hydrogen-bonded in a staggered array and conform to a common supercoil axis, such arrangements are not observed

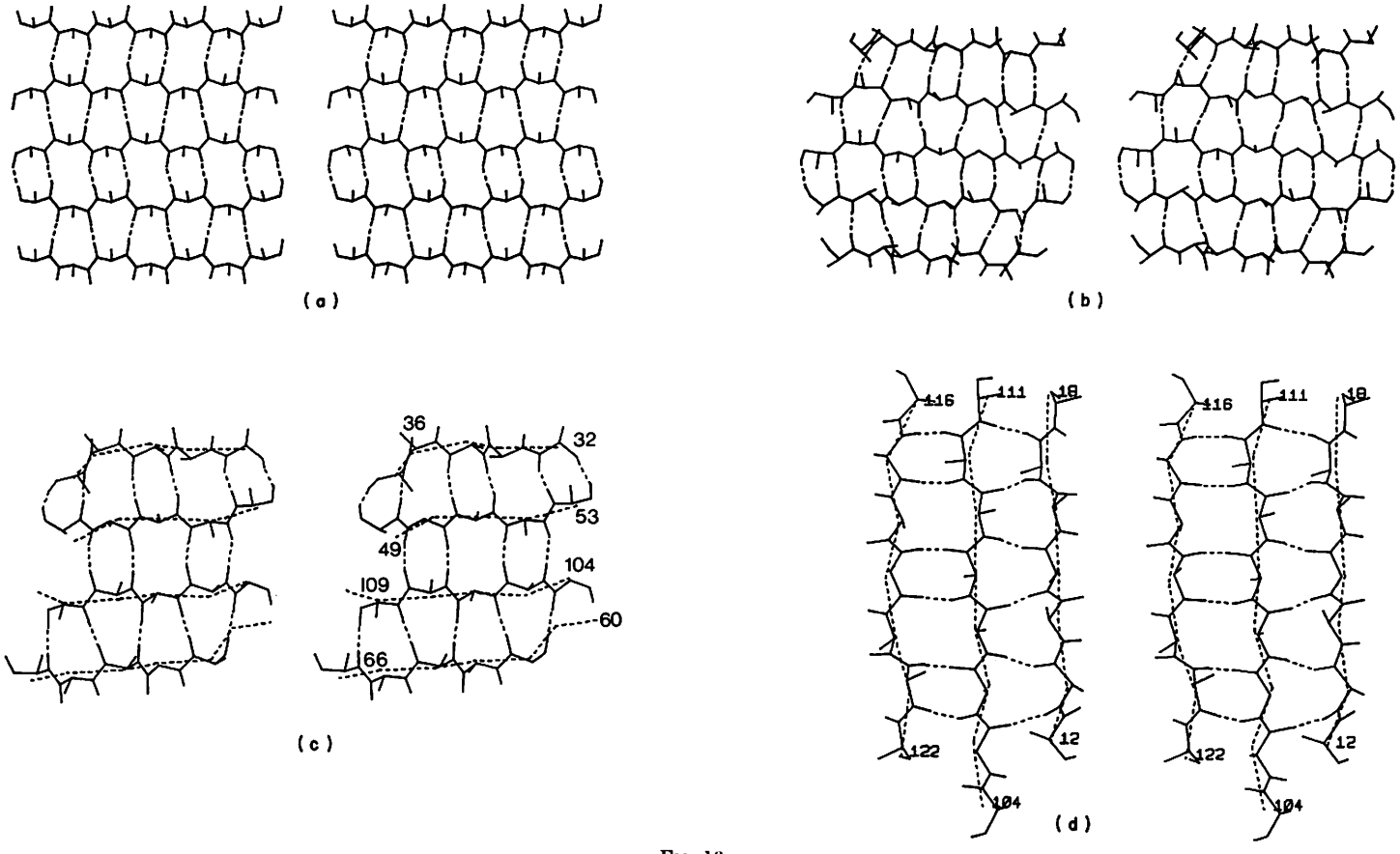

FIG. 16.

in known protein structures. Attempts to generate structures having six to eight conformationally regular strands, and at least four extended interchain hydrogen bonds failed to produce barrels that closed and had acceptable interchain hydrogen bonding. This result appears consistent with the observed properties of the previously described extended sheet structures, whose extended coiled-coil regions generally conform to cylindrical surfaces whose effective radius of curvature is too large to effect cyclic closure. Figure 15 shows views of a representative antiparallel β-barrel in α-chymotrypsin (Birktoft & Blow, 1972). As shown, closure of the structure necessitates the introduction of one or more β-bulges in order to attain the extent of chain twist required for barel closure. Note additionally that the chains of the structure tend to diverge spatially towards the ends of the barrel, whereas a hypothetical barrel structure composed of regular coiled-coils chains would ideally conform to a cylindrical surface of constant circular cross-section.

(c) *Mixed β-sheets*

The dipeptide repeat periods of the classical ($\delta = 180$, $\phi = -147°$, $\psi = 145$) antiparallel and parallel β-sheets differ by approximately 0·5 Å, a situation that precludes the formation of regular extended hydrogen-bonded interactions between them. However, as shown in Figure 3, the period of the antiparallel structure becomes shorter with the introduction of symmetrical hydrogen-bond bending at the carbonyl oxygen atoms. For a value of $\delta = 153°$, the local conformation of the parallel strands can be made identical to that of the antiparallel structure ($\phi = -116°$, $\psi = 112°$), thus allowing the formation of a perfectly hydrogen-bonded, mixed flat structure (Fig. 16(a)). As described previously, this conformation is not sterically allowed for amino acids substituted at Cα. However, if this structure twists in response to the minimization of the backbone conformational potential energy, an acceptable structure may be attained. This is a result of the increase in the repeat period that accompanies twisting of parallel

---

FIG. 16. Mixed β-sheets. (a) A flat mixed β-sheet ($\phi = -116°$, $\psi = 112°$) with $\delta = 153°$ for antiparallel strands of the sheet, and N–O hydrogen bond length of 2·8 Å. This perfectly hydrogen-bonded arrangement involves a sterically unfavorable contact for the Cβ atoms in the small hydrogen-bonded rings of the antiparallel sheet (Fig. 4). This sterically unfavorable interaction is relieved when the mixed sheet is twisted. (b) A crossing chain mixed, twisted ($\theta = -19·3°$) β-sheet with $\delta = 165°$ for parallel strands, $\phi = -114°$, $\psi = 128°$. Mean hydrogen bond length is 2·77 Å with a standard deviation of 0·41 Å. (c) Least-squares superposition of a regularized model with a mixed β-sheet region in carboxypeptidase A (broken lines). Parallel strands have straight helical conformations ($\phi = -114°$, $\psi = 120°$), whereas the exterior antiparallel strands are best approximated as slightly twisted coiled-coils with $\phi_1 = -118°$, $\psi_1 = 144°$, $\phi_2 = -100°$, $\psi_2 = 124°$ for residues 32 to 36, and $\phi_1 = -110°$, $\psi_1 = 126°$, $\phi_2 = -108°$, $\psi_2 = 118°$. Least-squares optimization of hydrogen bonds between these conformationally regular chains yields an extended model structure that gives an average superposition error of 0·54 Å for corresponding α-carbon atoms in the model and observed structures. The average hydrogen bond length in the model is 2·78 Å with a standard deviation of 0·18 Å. (d) A model fit to a mixed, triple-strand helicoid β-sheet in prealbumin (broken lines). The central chain has straight helical conformation ($\phi = -113°$, $\psi = 122°$), while the parallel (residues 12 to 18, $\phi_1 = -122°$, $\psi_1 = 134°$, $\phi_2 = 114°$, $\psi_2 = 140°$) and antiparallel (residues 116 to 122, $\phi_1 = -119°$, $\psi_1 = 134°$, $\phi_2 = 109°$, $\psi_2 = 128°$) exterior chains are regular coiled-coils. Least-squares optimization of the interchain hydrogen bonding produces an extended model with an average superposition error of 0·54 Å with the observed α-carbon positions. The average hydrogen bond length in the model is 2·77 Å with a standard deviation of 0·25 Å.

sheets (see Fig. 2 of Salemme & Weatherford, 1981), so that twisted parallel strands can potentially interact with longer period, less sterically hindered, antiparallel chains.

Figure 16(b) shows an example of model twisted, mixed β-sheet composed of straight-helical chains. Figure 16(c) shows a model fit to a mixed sheet region in carboxypeptidase A (Ludwig *et al.*, 1967). The exterior pair of antiparallel strands in this structure are best approximated as coiled-coils, since there is no external geometrical constraint at the edge of the sheet. Figure 16(d) shows a model fit to a triple-strand helicoid sheet in prealbumin (Blake *et al.*, 1974). Both of these sheets manifest the conformational flexibility inherent in the antiparallel structure, which allows it to adapt to the more rigidly specified geometries of twisted parallel sheets.

4. Conclusion

Examination of the conformational behavior of antiparallel β-sheets shows them to be quite flexible structures. This behavior is basically a result of the geometrical and symmetrical properties of the antiparallel structure, which admit a variety of possible chain conformations having similarly distorted hydrogen-bonding interactions. As a consequence, the observed geometrical configurations of antiparallel sheets frequently exhibit continuously deformed spatial configurations that reflect the effects of the interaction of the geometrical requirements for interchain hydrogen bond preservation, and local and long-range packing interactions.

This research was supported by grants from the National Institutes of Health (GM21534 and GM25664), the University of Arizona Computer Center, and a Dreyfus Teacher-Scholar Grant (to F.R.S.).

REFERENCES

Bernstein, F. C., Koetzle, T. F., Williams, G. J. B., Meyer, E. F. Jr, Brice, M. D., Rodgers, J. R., Kennard, O., Shimanouchi, T. & Tasumi, M. (1977). *J. Mol. Biol.* **112**, 535–542.

Birktoft, J. J. & Blow, D. M. (1972). *J. Mol. Biol.* **68**, 187–240.

Blake, C. C. F., Gelsow, M. J., Swan, I. D. A., Rerat, C. & Rerat, B. (1974). *J. Mol. Biol.* **88**, 1–12.

Buehner, M., Ford, G. C., Moras, D., Olsen, K. W. & Rossmann, M. G. (1974). *J. Mol. Biol.* **90**, 25–49.

Dickerson, R. E. & Geis, I. (1969). In *The Structure and Action of Proteins*, pp. 24–43, W. A. Benjamin, Menlo Park.

Feldman, R. J. (1976). *Atlas of Macromolecular Structure on Microfiche*, Tracor-Jitco, Rockville.

Hagler, A. T., Lifson, S. & Huler, E. (1974). In *Peptides, Polypeptides, and Proteins* (Blout, E. R., Bovey, F. A., Goodman, M. & Lotan, N., eds), pp. 35–48, Wiley Interscience, New York.

Hardman, K. D. & Ainsworth, C. F. (1972). *Biochemistry*, **11**, 4910–4919.

Huber, R., Kukla, D., Ruhlumann, A. & Steigemann, W. (1972). *Cold Spring Harbor Symp. Quant. Biol.* **36**, 141–150.

Ludwig, M. L., Hartsuck, J. A., Steitz, T. A., Muirhead, H., Coppola, J. C., Reeke, G. N. & Lipscomb, W. N. (1967). *Proc. Nat. Acad. Sci., U.S.A.* **57**, 511–514.

Matthews, B. W., Fenna, R. E., Bolognesi, M. C., Schmid, M. F. & Olson, J. M. (1979). *J. Mol. Biol.* **131**, 259–285.
Nishikawa, K. & Scheraga, H. (1976). *Macromolecules*, **9**, 395–401.
Pauling, L. & Corey, R. B. (1951). *Proc. Nat. Acad. Sci., U.S.A.* **37**, 729–740.
Raghavendra, K. & Sasisekharan, V. (1979). *Int. J. Pept. Protein Res.* **14**, 326–338.
Reeke, G. N. Jr, Becker, J. W. & Edelman, G. M. (1975). *J. Biol. Chem.* **250**, 1525–1547.
Richardson, J. S. (1977). *Nature (London)*, **268**, 495–500.
Richardson, J. S., Getzoff, E. D. & Richardson, D. C. (1978). *Proc. Nat. Acad. Sci., U.S.A.* **75**, 2574–2578.
Salemme, F. R. & Weatherford, D. W. (1981). *J. Mol. Biol.* **146**, 101–117.